

Experimental research on performances of the imaging plates applied in gamma-ray imaging^{*}

QI Jian-Min(祁建敏)¹ ZHANG Fa-Qiang(章法强) CHEN Jin-Chuan(陈进川) XIE Hong-Wei(谢红卫)

Institute of Nuclear Physics and Chemistry, China Academy of Engineering Physics, Mianyang 621900, China

Abstract: Experimental studies on the basic characteristics of IPs applied in γ -ray imaging are carried out by utilizing isotopic γ -ray sources. The 1.25 MeV γ -ray sensitivity of the BAS-MS and BAS-TR imaging plates and their enhanced sensitivity by covering appropriate Compton conversion foils are measured based on the studies of the image intensity linear calibration, time attenuation laws and the influence of scanning parameter settings. The energy-dependent γ -ray sensitivity of the IPs is also obtained by the studies of the measured sensitivity and the Monte Carlo simulated energy deposition in the IPs' sensitive layer. Furthermore, a method of a sandwich detection structure as well as its primary experimental validations are presented in order to increase the gamma-to-neutron ratio in a γ/n mixed radiation field.

Key words: gamma-ray imaging, imaging plate, linear calibration, time attenuation, gamma-ray sensitivity

PACS: 29.40.Gx, 81.70.Fy **DOI:** 10.1088/1674-1137/38/1/016001

1 Introduction

An imaging plate (IP) is a novel record medium for radiation imaging [1]. The radiation information is recorded in the phosphor sensitive layer of IPs in terms of quasi-steady state electrons and the subsequent outputs when quasi-steady state electrons are scanned by a 633 nm laser. Compared with a γ -ray imaging system composed of scintillators and a charged coupled device (CCD) camera coupled with a micro-channel plate (MCP), the IPs have good performances, such as high spatial resolution [2], large dynamic range [3], good response to a flat radiation field, large sensitive area [4] and insensitive to electromagnetic radiation, etc. It can therefore be used as a recording unit for either γ -ray imaging in inertial confinement fusion (ICF) experiments and nondestructive testing or precise calibration of a γ -ray imaging system, such as descriptions of radiation sources, studies of the collimator imaging characteristics and measurements of the spatial point spread function (PSF) and resolution of the system, etc.

Original output images of the IPs are non-linear, measuring in a unit called 'quantum level' (QL). These non-linear images need to be converted to images of which the intensity is linear with the integrated radiant intensity or dose. Ref. [5] proposes a formula for converting the non-linear unit 'QL' to a linear unit 'PSL'

(photo-stimulated luminescence). Comparing with our measurements, the formula fits well with the experimental results in the low radiation flux region, but is not perfect in the high radiation flux region. Thus, linear intensity calibration of the IPs' output images has been carried out utilizing several isotopic γ -ray sources, in order to understand the linear conversion principles of the original non-linear images. Moreover, the time attenuation curves of different types of IPs and the influence of scanning parameter settings over image intensity and signal-to-noise ratio (SNR) are investigated.

IPs are broadly applied in X-ray [6], charged particle [7, 8] and thermal neutron [9, 10] imaging. However, reports about the γ -ray and fast neutron imaging are comparatively few, since the γ -ray sensitivity of IPs is low and statistical fluctuation of the image intensity is comparatively high. On the other hand, theoretically calculated results indicate that the energy depositions of both γ -rays and neutrons with energies of several MeV are almost the same. In order to apply γ -ray imaging in a γ/n mixed radiation field, the IP's γ -ray sensitivity needs to be improved to increase the γ -ray imaging quality, such as statistical fluctuation and the gamma-to-neutron ratio. Methods of increasing the γ -ray sensitivity by covering appropriate Compton conversion foils on the IP surface and a sandwich detection structure, as well as primary experimental validations, are presented.

Received 25 January 2013

^{*} Supported by Youth Foundation of NNSF (11005095) and Science and Technology Development Foundation of China Academy of Engineering Physics (2011B0103017)

1) E-mail: qjm06@sina.com

©2014 Chinese Physical Society and the Institute of High Energy Physics of the Chinese Academy of Sciences and the Institute of Modern Physics of the Chinese Academy of Sciences and IOP Publishing Ltd

2 Experimental studies on the basic characteristics of IPs

2.1 Linear intensity calibration of the IP image

The relation between the γ -ray radiant intensity and the IP image intensity is measured using a ^{137}Cs isotopic source, which emits 0.662 MeV γ -rays. A BAS-MS type IP (Fuji film Com. Ltd.), which has a 9 μm protective Mylar layer and a 115 μm sensitive layer, and a Typhoon FLA7000 IP scanner are employed. The integrated γ -ray radiant intensity is adjusted by changing the irradiating time, keeping the IP in the same position during the experiments.

The original image intensity of BAS-MS IP in the 'QL' unit (ranging from 0 to 65535) varies with different radiant intensities is illustrated in Fig. 1. The scanning pixel size is chosen to be 100 μm and the scanner PMT voltage is set to 900 V. The measured data are fitted by a power function with a power law index of 0.518 ± 0.009 . Therefore, we choose a new image intensity unit, 'counts', (ranging from 0 to 100000) instead of the unit 'PSL'. As is shown in Fig. 2, the image intensity with our unit of 'counts' has a good linear relationship with the γ -ray radiant intensity in a large dynamic range from a low γ -ray flux of $\sim 10^6 \text{ cm}^{-2}$ to an almost saturated γ -ray flux of $\sim 10^9 \text{ cm}^{-2}$. On condition of current scanner settings, the image intensity unit 'counts' and 'QL' obey the following law:

$$\text{counts} = 2.3284 \times 10^{-5} \cdot \text{QL}^2, \quad (1)$$

where the coefficient is determined by the scanner parameter settings.

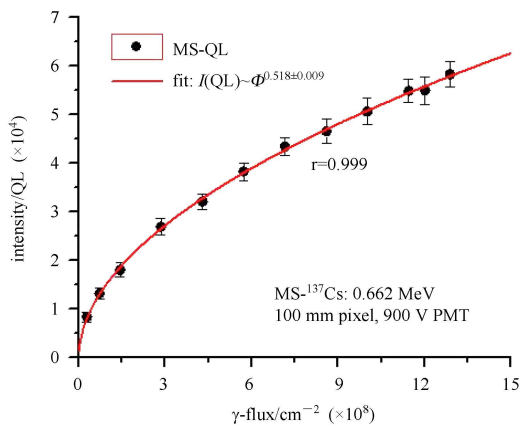


Fig. 1. The original image intensity of the BAS-MS IP varies with the γ -ray radiant intensity.

2.2 Measurements of the IPs' time attenuation curves

Some electrons in the IP's sensitive phosphor layer

save the deposited radiation energy in the form of a quasi-steady state. The phenomenon that the image intensity gradually decreases with the increase of the time interval between irradiating and scanning is described as a time attenuation curve, since the quasi-steady state electrons are de-excited because of the thermal movements. The time attenuation curve can be expressed by an exponential function with fast and slow components, which are determined by IP types and environmental temperatures but are independent of radiation type or intensity.

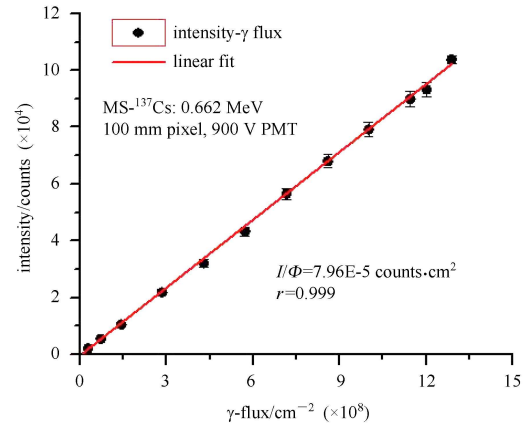


Fig. 2. The linear image intensity calibration of the BAS-MS IP varies with the γ -ray radiant intensity.

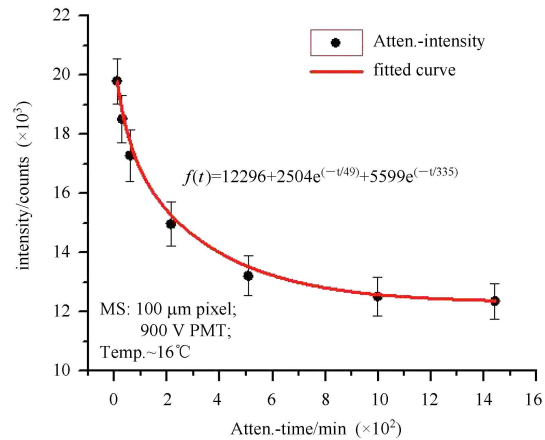


Fig. 3. The measured time attenuation curve of BAS-MS IPs.

The time attenuation curves of BAS-MS and BAS-TR (with no protective layer and the sensitive layer thickness is 52 μm) are illustrated in Fig. 3 and Fig. 4, respectively. The IP is irradiated by the ^{137}Cs γ -ray source for 100 s. The attenuation time is chosen to be from 15 min to 24 h and the environmental temperature is kept to be 15–18 $^{\circ}\text{C}$. The measured fast and slow attenuation time constants of BAS-MS IPs are 49.7 min and

335 min respectively, while the relevant values presented in Ref. [11] are 48 min and 288 min. The measured fast and slow attenuation time constants of BAS-TR IP are 48 min and 295 min, respectively. If the BAS-TR IP's time attenuation curve is fitted by a power function ax^b , then the power law index b is fitted to be -0.10 , while the relevant value obtained in an environment with a temperature of 21 ± 1 °C (which brings the main differences) is -0.14 [5]. The uncertainty of the fitted parameters is estimated to be 10%–15%.

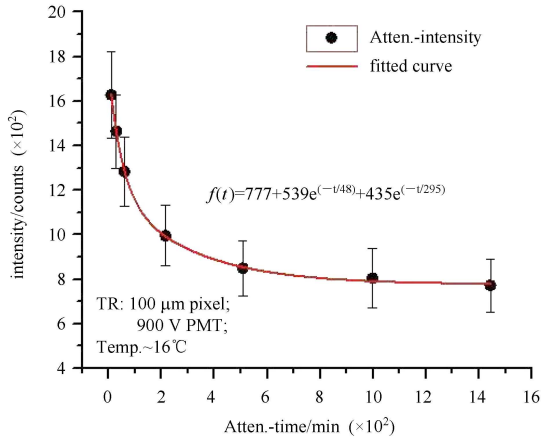


Fig. 4. The measured time attenuation curve of BAS-TR IPs.

2.3 Influence of the scanner settings over the IP's image intensity

The IP's image intensity partially depends on the scanner parameter settings, in which the scanning pixel size and the scanner PMT voltage play a most important role. Thus the image intensity and signal-to-noise ratio (SNR) are studied under the same irradiating conditions when different scanning settings are chosen.

The scanning pixel size determines the basic spatial resolution of the IP images. The measured image intensity and SNR corresponding to different scanning pixel sizes are illustrated in Fig. 5. The results indicate that

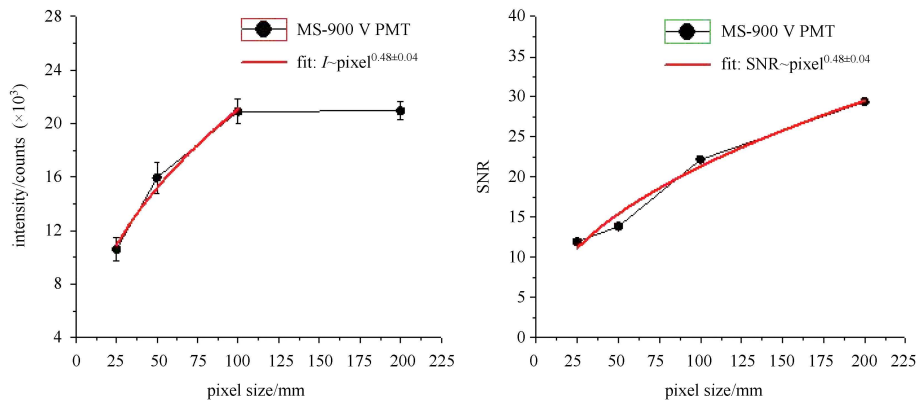


Fig. 5. The IP's image intensity and SNR vary with scanning pixel sizes.

the image intensity and SNR have a direct ratio with the square root of scanning pixel sizes, except for that the image intensity is kept the same when the scanning pixel size increases from 100 μm to 200 μm. The latter has been repeated many times in experiments and is confirmed by the same results. It is possibly related to the procedures of laser scanning and luminescence collecting, which need further study.

The scanner sensitivity depends on the PMT voltage, which determines the output image intensity (shown in Fig. 6). The image intensity varies with the sixth power of the PMT voltage when the image SNR remains unchanged, since the latter is determined by the statistical fluctuation of the image intensity.

3 Experimental studies on γ -ray sensitivities of the IPs

3.1 The γ -ray sensitivity and methods to improve the sensitivity

The IPs' γ -ray sensitivity measurements are accomplished on a ^{60}Co isotopic source, which emits γ -rays with an energy of about 1.25 MeV. During the complete measurement procedure, the image intensity is revised by the time attenuation curve based on time intervals between irradiating and scanning.

Figure 7 illustrates the measured 1.25 MeV γ -ray sensitivity of both the BAS-MS and BAS-TR IPs scanned with parameters of 100 μm pixel size and 900V PMT voltage. The measured 1.25 MeV γ -ray sensitivity of BAS-MS IP is 5.54×10^{-5} counts·cm $^{-2}$ and the dynamic range is from 9×10^6 cm $^{-2}$ to 1.8×10^9 cm $^{-2}$ with a relevant intensity value of approximately 500–100000 counts. The measured 1.25 MeV γ -ray sensitivity of BAS-TR IP is 5.92×10^{-6} counts·cm $^{-2}$ and the dynamic range is from 2.7×10^7 cm $^{-2}$ to 1.69×10^{10} cm $^{-2}$ with a relevant intensity value of approximately 200–100000 counts. The lower limits of both the BAS-MS and BAS-TR IPs' dynamic range are determined according to SNR=2.

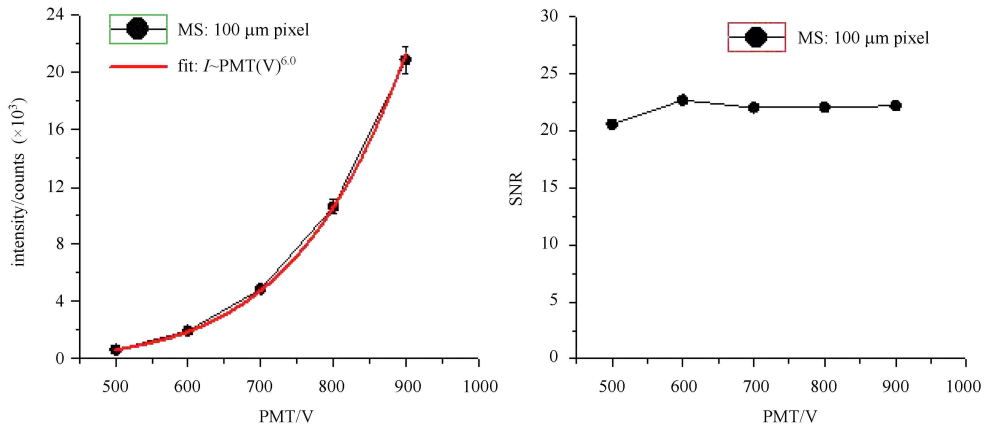


Fig. 6. The IP's image intensity and SNR vary with the scanner's PMT voltage.

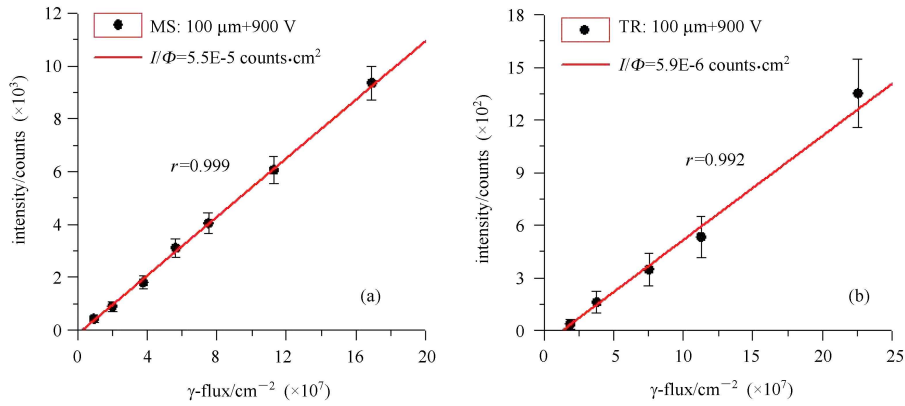


Fig. 7. The measured 1.25 MeV γ -ray sensitivity of BAS-MS IP (a) and BAS-TR IP (b).

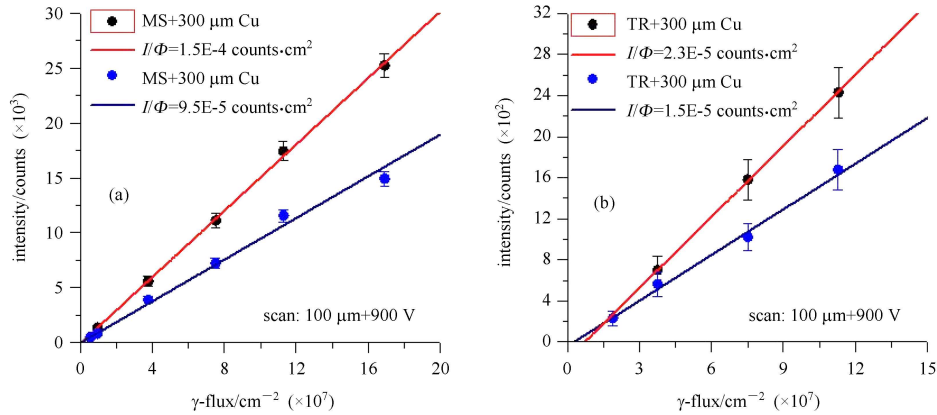


Fig. 8. The enhanced 1.25 MeV γ -ray sensitivity of BAS-MS IP (a) and BAS-TR IP (b).

The IP's sensitive phosphor layer is only about 100 μm thick and the energy deposition of γ -rays with an energy of several MeV is quite small. Thus a high radiant intensity ($\sim 10^8$ cm^{-2}) needs to be integrated to obtain signals with appropriate SNR. Therefore, a method of covering Compton conversion foils on the IP surface is proposed. The γ -ray sensitivity of the IPs

can be improved by the Compton electrons produced in the foils by interactions between γ -rays and metal atoms. As is shown in Fig. 8, the measured 1.25 MeV γ -ray sensitivity is increased to 9.47×10^{-5} counts. cm^2 and 1.51×10^{-4} counts. cm^2 for BAS-Ms IP and while employing a 130 μm and 300 μm Cu foil, respectively. The measured 1.25 MeV γ -ray sensitivity of

BAS-TR IP is increased to 1.48×10^{-5} counts·cm² and 2.30×10^{-5} counts·cm² for BAS-TR IP while employing a 130 μm and 300 μm Cu foil, respectively.

The 1.25 MeV γ-ray sensitivity of BAS-MS IP varying with Cu foil thickness are calculated by a GEANT4 Monte Carlo code. As is shown in Fig. 9, the calculated and measured sensitivities are perfectly consistent with each other. Moreover, the calculations indicate that the influence of covering 100–300 μm Cu foils on the IP surface on the spatial resolution of γ-ray imaging in an energy range from 0.75 MeV to 3.0 MeV is only 20–50 μm.

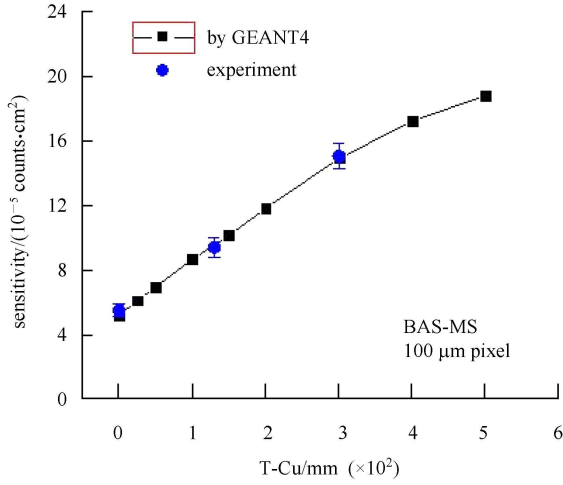


Fig. 9. The calculated and measured 1.25 MeV γ-ray sensitivities of BAS-MS IP varying with the Cu foil thickness.

3.2 Primary studies on a sandwich detection structure of IPs

In the mixed γ-ray/neutron radiation fields, the IP image contains the contributions of both the γ-rays and neutrons. A sandwich detection structure composed of a double IPs filling with a Cu foil is created to improve the γ-ray to neutron sensitivity ratio of γ-ray images through subtracting the front IP image from the rear IP

image. Fig. 10 illustrates the primary experimental results of the detection structure filling with a 130 μm Cu foil. The 1.25 MeV γ-ray sensitivity of the front BAS-MS IP is 4.2×10^{-5} counts·cm² and the relevant value of rear IP is 1.0×10^{-4} counts·cm², which is 2.3 times the front IP. The images obtained through subtracting the front IP image from the rear IP image reflect only the Compton interactions between the incident γ-rays and the Cu conversion foil, thus the influence of neutrons and scattered γ-ray background can be greatly reduced. Further studies will be put forward to consummate the method.

4 Simulation of the energy-dependent IPs' γ-ray sensitivity

The average γ-ray energy deposition E_{dep} (eV/photon) in both BAS-MS and BAS-TR IPs is calculated using a GEANT4 Monte Carlo code (Fig. 11). A conversion formula between the BAS-MS IP's sensitivity to γ-rays of various energy $S(E_\gamma)$ and relevant $E_{\text{dep}}(E_\gamma)$ can be obtained by comparing the measured 1.25 MeV γ-ray sensitivity and the calculated 1.25 MeV γ-ray energy depositions:

$$S(E_\gamma) = \frac{I(\text{counts})}{\Phi_\gamma(\text{cm}^{-2})} = E_{\text{dep}}(E_\gamma) \cdot 3.73 \times 10^{-7}, \quad (2)$$

where the coefficient is determined by the IP type and the scanning parameters of 100 μm pixel size and 900V scanner PMT voltage. The other experimental data, such as BAS-MS IP's 0.662 MeV γ-ray sensitivity and its 1.25 MeV γ-ray sensitivity covered with a 300 μm Cu foil, are subsequently converted to energy depositions and are illustrated in Fig. 11. The calculated and measured results have good consistency.

From the data of the BAS-TR IPs, it is obtained

$$S(E_\gamma) = \frac{I(\text{counts})}{\Phi_\gamma(\text{cm}^{-2})} = E_{\text{dep}}(E_\gamma) \cdot 1.50 \times 10^{-7}. \quad (3)$$

The 1.25 MeV γ-ray sensitivity of the BAS-TR IP cov-

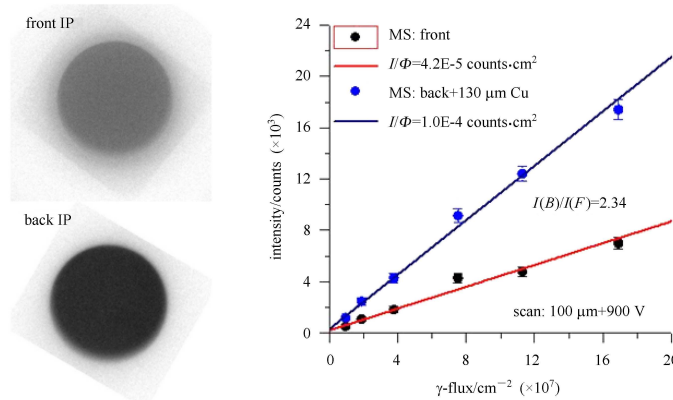


Fig. 10. The measured 1.25 MeV γ-ray sensitivities of a sandwich structure filling with a 130 μm Cu foil.

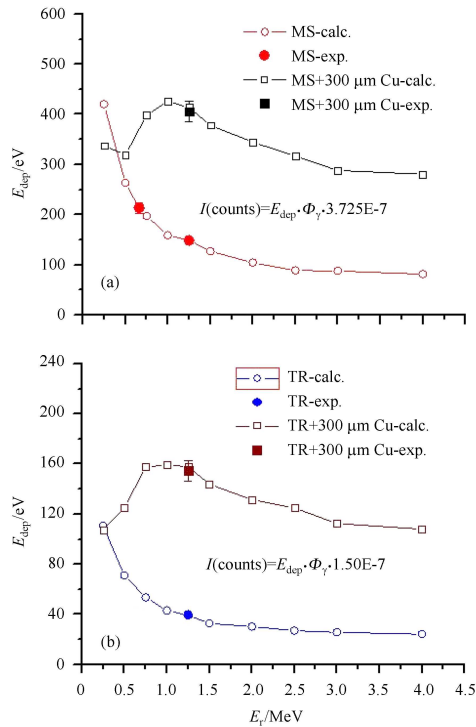


Fig. 11. The simulated and measured γ -ray energy deposition in BAS-MS (a) and BAS-TR (b) IPs.

ered with a 300 μm Cu foil is converted to energy deposition by the above formula and illustrate the result in Fig. 11. The calculated and measured results also show a good consistency.

Formula (2) and formula (3) have different coefficients. This is because, on one hand, the sensitive layer of BAS-TR IPs is relatively thin (52 μm) and is dyed with blue to reduce the scanning laser dispersion, which is unlike the BAS-MS IPs. On the other hand, the laws about the incidence of scanning laser and emission of the photo-stimulated luminescence in both types of IPs are quite different.

As is shown in Fig. 11, both the BAS-MS and BAS-TR IPs' sensitivities to γ -rays with energy above 1.0 MeV are increased by time when covered with 300 μm Cu foils. Hence the energy response curve of the IP's

γ -ray sensitivity becomes comparatively flat, which is helpful to improve the signal-to-background ratio (SBR) of γ -ray imaging.

5 Conclusions

The imaging plate has good performance suitable for radiation imaging and can be used as a recording unit for either γ -ray imaging or the precise calibration of a γ -ray imaging system. Experimental studies on the basic characteristics of the IPs applied in gamma-ray imaging are carried out by utilizing isotopic γ -ray sources. A linear image intensity unit, 'count', is chosen by experimental studies on the relationship between the original image intensity and the γ -ray radiant intensity. The time attenuation curves of both the BAS-MS and BAS-TR IPs corresponding to an environmental temperature of $\sim 16^\circ\text{C}$ are measured, in which the time attenuated constants are consistent with results from relative work. The image intensity and its SNR under different scanning parameter settings are also studied. The 1.25 MeV γ -ray sensitivity of BAS-MS and BAS-TR IPs and their enhanced sensitivity by covering appropriate Compton conversion foils are measured. When a 900V PMT voltage and a 100 μm pixel size are selected, the 1.25 MeV γ -ray dynamic range of BAS-MS IPs is from $9 \times 10^6 \text{ cm}^{-2}$ to $1.8 \times 10^9 \text{ cm}^{-2}$, while the relevant dynamic range of BAS-TR IPs is from $2.7 \times 10^7 \text{ cm}^{-2}$ to $1.69 \times 10^{10} \text{ cm}^{-2}$. The 1.25 MeV γ -ray sensitivity of IPs can be increased by almost 3 times by covering a 300 μm Cu foil. In addition, a sandwich detector is proposed and the primary experimental results show that it increases the gamma-to-neutron sensitivity ratio in a γ/n mixed radiation field. The energy response to γ -ray sensitivity of the IPs is also obtained by the studies of the measured sensitivity and the Monte Carlo simulated energy deposition in the IPs' sensitive layer. The energy response curves of IPs become 'flat' when covering appropriate Cu foils, thus high energy γ -ray imaging signals are enhanced and the signal-to-background ratio is improved. Application of IPs in γ -ray and fast neutron imaging will be carried out in future work.

References

- 1 Villers D, Paternostre L, Dosière M et al. Nucl. Instrum. Methods B, 1995, **97**(1-4): 265-268
- 2 Yamamoto Masaki, Kumasaka Takashi, Uruga Tomoya et al. Nucl. Instrum. Methods A, 1998, **416**(2-3): 314-318
- 3 Hiroko Ohuchi, Yasuhiro Kondo. Nucl. Instrum. Methods A, 2010, **621**(1-3): 468-472
- 4 Yoshiyuki Amemiya. Methods in Enzymology, 1997, **276**: 233-243
- 5 Paterson J I, Clarke J R, Woolsey C N et al. Meas. Sci. Technol., 2008, **19**: 095301
- 6 Gales S G, Bently C D. Rev. Sci. Instrum. A, 2004, **75**(10): 4001-4003
- 7 Doyama Masao, Takano J, Inoue M et al. Nucl. Instrum. Methods A, 1997, **394**(1-2): 146-150
- 8 Nohtomi A, Terunuma T, Kohno R et al. Nucl. Instrum. Methods A, 1999, **424**(2-3): 569-574
- 9 Takahashi Kenji, Tazaki Seiji, Miyahara Junji et al. Nucl. Instrum. Methods A, 1996, **377**(1): 119-122
- 10 Nares Chankow, Suvit Punnachaiya, Sarinrat Wonglee. Applied Radiation and Isotopes, 2010, **68**(4-5): 662-664
- 11 Zeil K, Kraft S D, Jochmann A et al. Rev. Sci. Instrum. A, 2010, **81**: 013307